Supporting information

Near-Infrared Fluorescence Energy Transfer Imaging of Nanoparticle Accumulation and Dissociation Kinetics in Tumor-Bearing Mice

Yiming Zhao,[1,2] Inge van Rooy,[2,3] Sjoerd Hak,[4] Francois Fay,[2] Jun Tang,[2,5] Catharina de Lange Davies,[6] Mihaela Skobe,[7] Edward Allen Fisher,[8] Aurelian Radu,[3] Zahi. A. Fayad,[2] Celso de Mello Donegá,[1] Andries Meijerink[1] and Willem J. M. Mulder[2,9]*

1. Condensed Matter and Interfaces, Debye Institute for Nanomaterials Science, Utrecht University, Princetonplein 5, 3584 CC Utrecht, The Netherlands.

2. Translational and Molecular Imaging Institute, Icahn School of Medicine at Mount Sinai, One Gustave L. Levy Place, New York, NY 10029, USA.

3. Developmental and Regenerative Biology, Icahn School of Medicine at Mount Sinai.

4. MI Lab and Department of Circulation and Medical Imaging, The Norwegian University of Science and Technology, Trondheim, Norway.

5. Graduate School of Biological Sciences, Icahn School of Medicine at Mount Sinai.

6. Department of Physics, The Norwegian University of Science and Technology, Trondheim, Norway.

7. Derald H. Ruttenberg Cancer Center, Icahn School of Medicine at Mount Sinai.

8. Langone Medical Center, New York University, New York, USA.

9. Department of Vascular Medicine, Academic Medical Center, Amsterdam, The Netherlands.

*Corresponding author information:
Willem Mulder, Ph.D.
willem.mulder@mssm.edu
Icahn School of Medicine at Mount Sinai
One Gustave L. Levy Place, Box 1234
New York, NY 10029
Ph. 212-824-8910

Supporting methods

Synthesis of near-infrared (NIR) emitting CdTe/CdSe/CdS/ZnS core-shell-shell (CSS)QDs.

CdTe/CdSe/CdS/ZnS core-shell-shell QDs were synthesized through a modified SILAR method.[1] Briefly, CdTe seed particles emitting at 576 nm were synthesized according to Wuister *et al*.[2] For multi-shell growth, washed CdTe cores were dispersed in 4 ml octadecene and 1.5 ml oleylamine. 20 mg tetradecylphosphonic acid was added as a stronger bonding ligand to maintain the spherical shape of the nanocrystal and to prevent Ostwald ripening. CdSe shell was grown by alternately adding 0.1 M cadmium oleate (made by dissolving CdO in oleic acid), and 0.1M Se in trioctylphosphine (TOP) as precursor solutions, and 0.1M S in TOP was used instead for subsquent CdS shell growth. The first layer of CdSe shell was grown at 200 °C, and temperature was then increased to 230 °C for later shell growth. The final ZnS shell was grown through adding 0.1M zinc diethyldithiocarbamate in TOP as single source precursor at 120 °C and by subsequently heating to 220 °C for shell growth. The emission wavelength was monitored through taking aliquots and measuring the sample emission spectra immediately after dispersion in toluene. The final emission wavelength was adjusted by stopping the precursor addition when desired wavelength was reached. The final product was washed in chloroform and acetone, and redispersed in chloroform.

Synthesis of Cy5.5-DMPE-labeled PEG-DSPE-coated quantum dot micelles (QD610-Cy5.5-PEG).

The 610 nm emitting CdSe/CdS/ZnS CSS quantum dots were synthesized according

to literature.[3] The emission wavelength was 610 nm and the size was around 7.5 nm determined by TEM. The QD610-Cy5.5-PEG micelles were synthesized using the same method as described above.

Optical characterization of nanoparticles

The emission spectra were recorded using a 450W Xe lamp as excitation source and a double grating 0.22 m SPEX monochromator of a SPEX Fluorolog to select the excitation wavelength of 500 nm. Emission was collected through an optical fiber leading to a 0.3 m monochromator (150 lines/mm, blazed at 550 nm) and detected by a liquid nitrogen cooled Princeton Instruments CCD camera (1024 × 256 pixels). Photoluminescence lifetime measurements were obtained by time-correlated single-photon counting. The setup consisted of a pulsed PicoQuant laser (2.5MHz, wavelength 406 nm), in combination with a monochromator (1350 lines/mm blazed at 630nm), a Hamamatsu photo-multiplier tube (H5738P-01), and a Time Harp 200 computer card.

Negative stain transmission electron microscopy (TEM)

The buffer of QD-Cy7-PEG solution was replaced by TEM buffer (0.125 M $CH_3CO_2NH_4$, 2.6 mM $(NH_4)_2CO_3$ 0.26 mM tetrasodium EDTA at pH 7.4) through washing twice in Vivaspin MWCO 30,000 centrifugation tubes. Samples were diluted to appropriate concentrations with TEM buffer and mixed with equal volumes of 2 % phosphotungstic acid (2PTA). The mixed solution was dropped and left to dry on a 100 mesh Formvar-coated nickel grid (Electron Microscopy Sciences). Sample grids were

examined using a Hitachi 7650 TEM coupled to a Scientific Instruments and Applications (SIA) digital camera controlled by Maxim CCD software at 80 kV.

Peri-tumor injection of nanoparticles and lymph node imaging.

Two groups of tumor mice (n = 3 animals for each group) were injected with two different nanoparticle solutions: (1) 10 μL of 20 nmol/ml QD710-Cy7-PEG; (2) 10 μL of 20 nmol/ml QD710 –PEG as the QD control. The solutions were injected intradermally in the peri-tumor region while the mice were under anesthesia. Immediately after injection, migration of the nanoparticles and dynamics of the lymphatic drainage were followed by fluorescence imaging in the three channels at 5 minute intervals for 1h. The injection spot was masked while imaging to prevent saturation of the signal due to the much greater brightness of the injection site compared to the lymphatic vessels and lymph nodes. In all cases, the nanoparticles drained to the left inguinal lymph node within minutes, and in some cases continued to migrate to the left axillary node. To confirm the nanoparticles' drainage to the sentinel lymph nodes, 1% Evans blue was also injected in the peri-tumor region. Mice were sacrificed at 5 h (n=3) or 45 h (n=3) after injection. The left side inguinal nodes and other major organs were harvested and subjected to fluorescence imaging immediately in the three optical channels.

Determination of circulation half-life of QD micelles in mice.

A group of 3 mice were injected intravenously with 100 pmol/g QD610-PEG. Blood samples were taken at 5, 10, 20, 30min, 1, 2, 4, and 8h after injection, through

puncturing the saphenous vein while mice were under anesthesia. At least 3 mg of blood was taken per sample and each sample was carefully weighed then diluted with 100 μL PBS. QD luminescence intensity was measured using IVIS imaging system.

Estimation of Förster distance

The Förster distance R_0 is the critical distance where the energy transfer rate equals the radiative decay rate of the donor. It can be calculated as

$$R_0 = \left(\frac{9000(\ln 10)\kappa_p^{\,2} Q_D}{N_A 128\pi^5 n_D^{\,4}} I \right)^{1/} \qquad (1)$$

where N_A is the Avogadro constant; κ_p^2 is the orientation factor and is usually assumed to be 2/3 as a random distribution; Q_D is the quantum yield of the QD donor; n_D is the refractive index of the medium; I is the spectra overlap(see Figure S2b). The R_0 of QD710-Cy7 donor-acceptor pair is calculated to be 6.9 nm.

SUPPORTING FIGURES

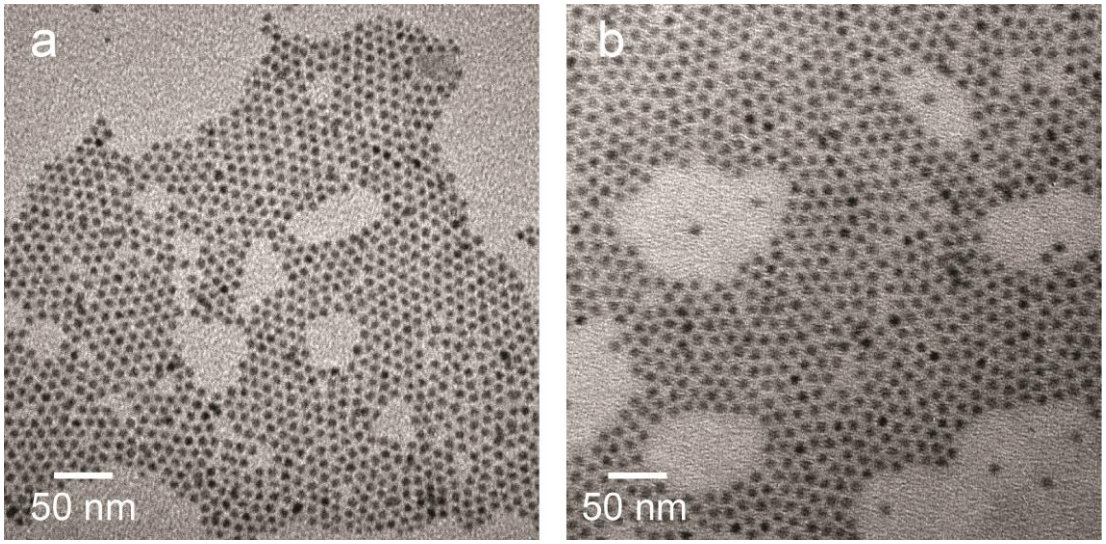

Figure S1. TEM images of (a) QD610 (CdSe/CdS/ZnS) and (b) QD710 (CdTe/CdSe/CdS/ZnS)

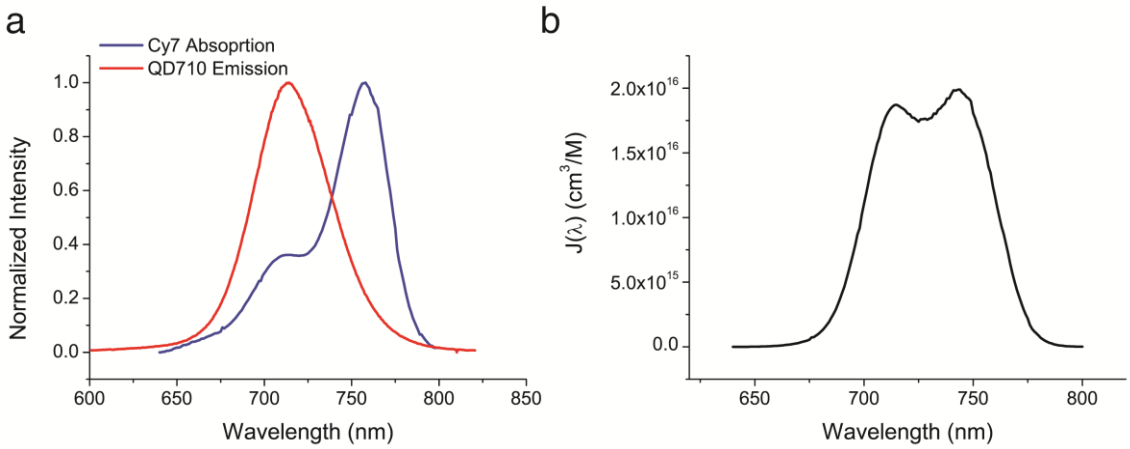

Figure S2 (a) Fluorescence emission spectrum of QD710 and absorption spectrum of Cy7 lipid. In order to calculate the Förster distance between QD710 and Cy7 lipid, overlap function J(λ) between QD emission and Cy7 lipid absorption is calculated.[4] $J(\lambda)=F_D(\lambda)\ \varepsilon_A(\lambda)\lambda^4$, where $F_D(\lambda)$ is dimensionless normalized donor emission spectrum, and $\varepsilon_A(\lambda)$ is extinction coefficient of acceptor. The results of J(λ) is presented in (b).

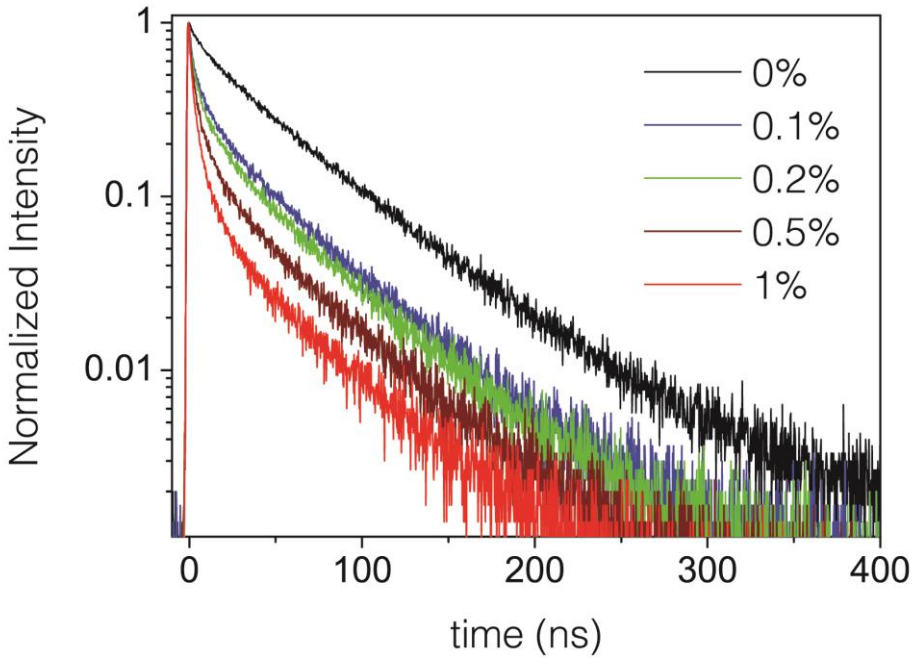

Figure S3. Fluorescence decay curve of QD emission at 710 nm from QD710-Cy7-PEG nanoparticles in PBS with indicated percentage of Cy7-lipids in the lipid corona. The nanoparticles were excited with a diode laser at 400nm. The gradual decrease of lifetime upon increase of Cy7-lipids confirms the occurrence of Förster resonance energy transfer (FRET).

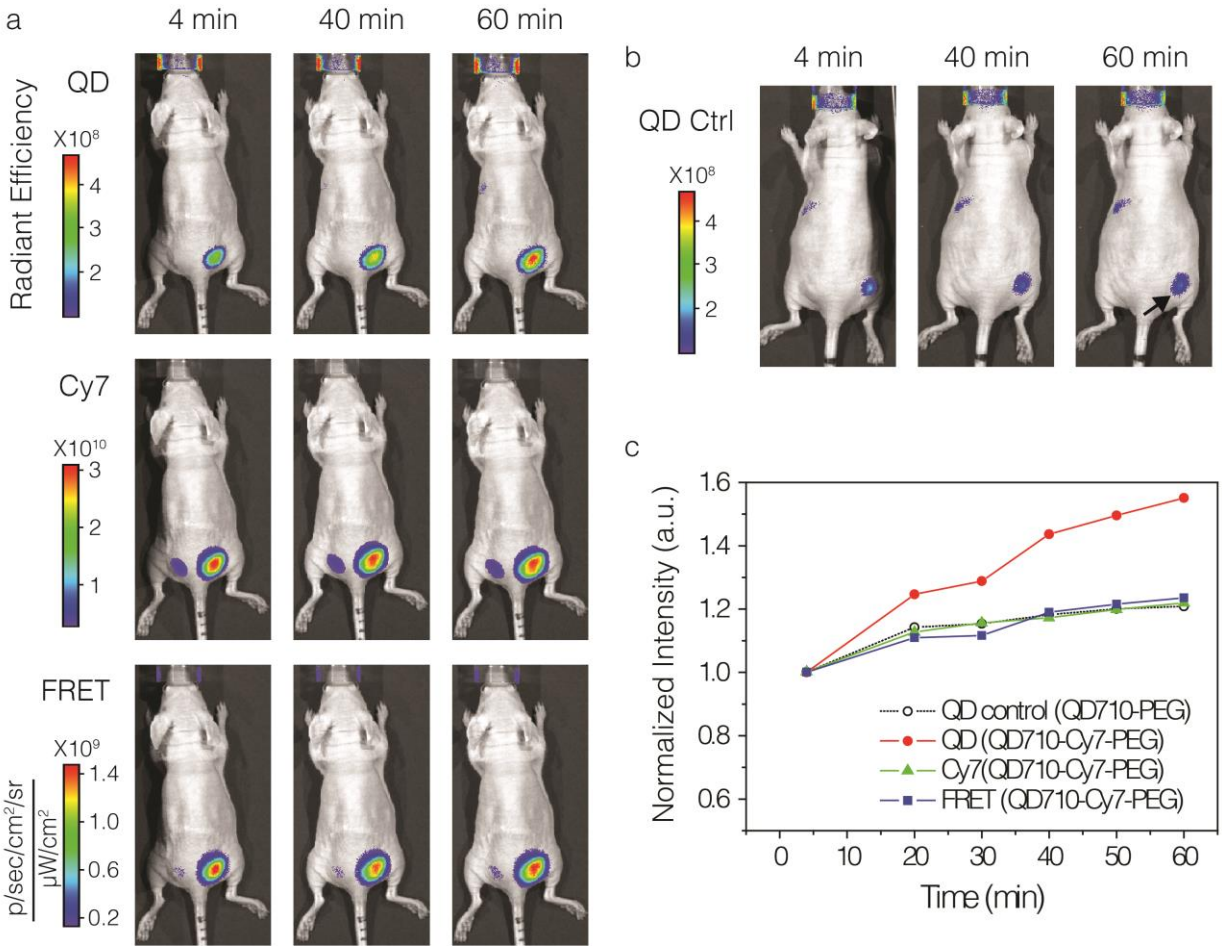

Figure S4. Test of FRET principle *in vivo*. **a**, NIR florescence image of nude mice at 4, 40, and 60min post-injection. The right side flank of the mice was subcutaneously injected with 5 pmol/g QD710-Cy7-PEG. Fluorescent signal was collected through three optical channels: QD (λ_{Exc} = 605 ± 18 nm, λ_{Em} = 720 ± 10 nm), Cy7 (λ_{Exc} =745± 18 nm, λ_{Em} = 800 ± 10 nm) and FRET (λ_{Exc}= 605± 18 nm, λ_{Em}= 800 ± 10 nm). **b**, Control mice subcutaneously injected with 2 pmol/g QD710-PEG in the right side flank **c.** The integrated luminescent intensities from the injected areas plotted against post-injection time. There is a gradual increase of intensity of about 20% within 1 h in all channels, due to diffusion of the nanoparticles from the injection site. However, the QD intensity from the FRET dots increased over 50% after 1 h. This enhancement of QD intensity is due to dissociation of Cy7-lipids which dequenches the QD emission.

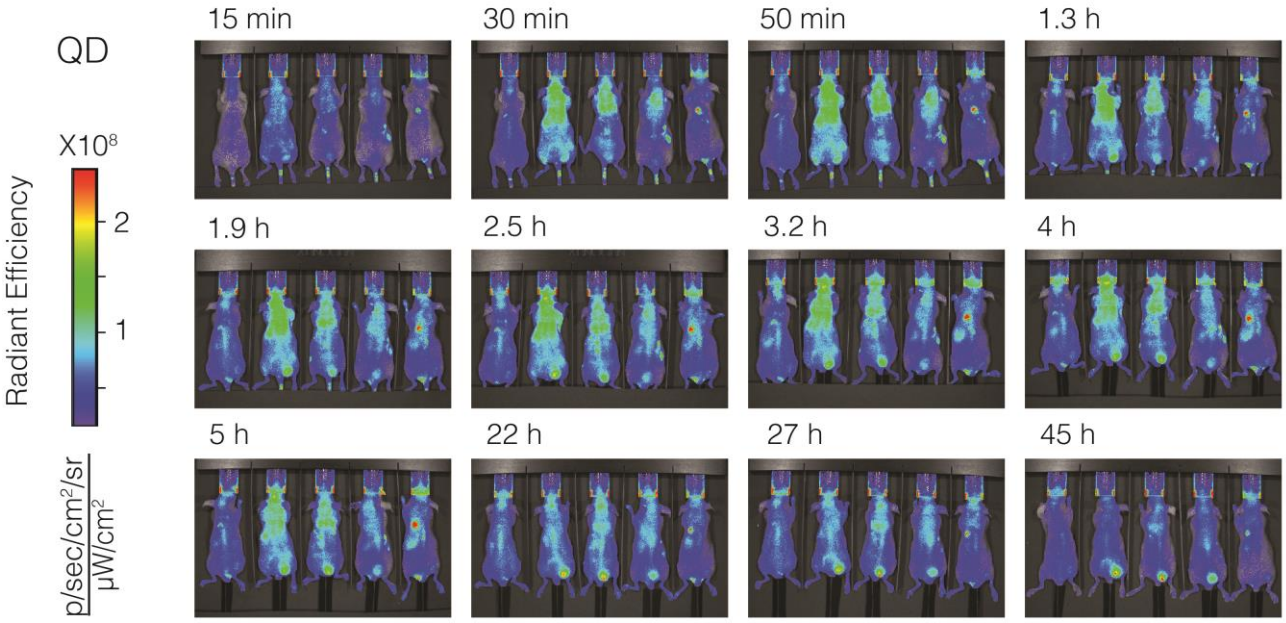

Figure S5. *in vivo* NIR florescence image of tumor-bearing mice intravenously injected with 100 pmol/g QD710-Cy7-PEG. At the indicated post-injection times, the fluorescence signal is collected through the QD channel (λ_{Exc} = 605 ± 18 nm, λ_{Em} = 720 ± 10 nm).

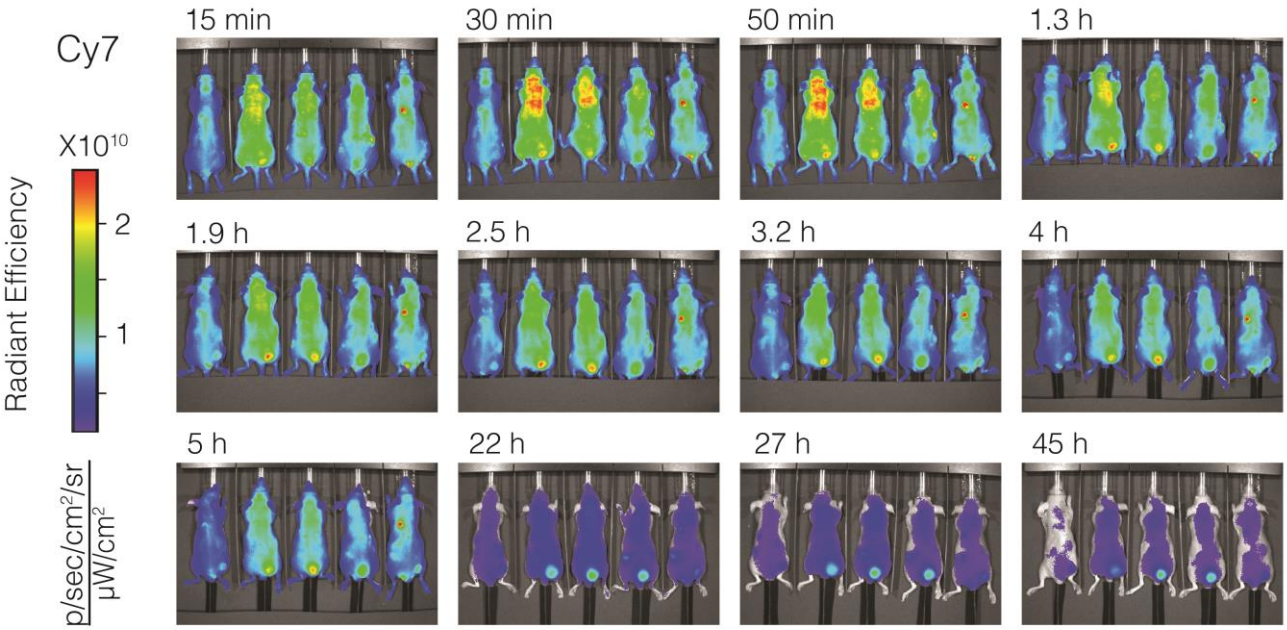

Figure S6. *in vivo* NIR florescence image of tumor-bearing mice intravenously injected with 100 pmol/g QD710-Cy7-PEG. At the indicated post-injection times, the fluorescence signal is collected through Cy7 channel (λ_{Exc} =745± 18 nm, λ_{Em} = 800 ± 10 nm).

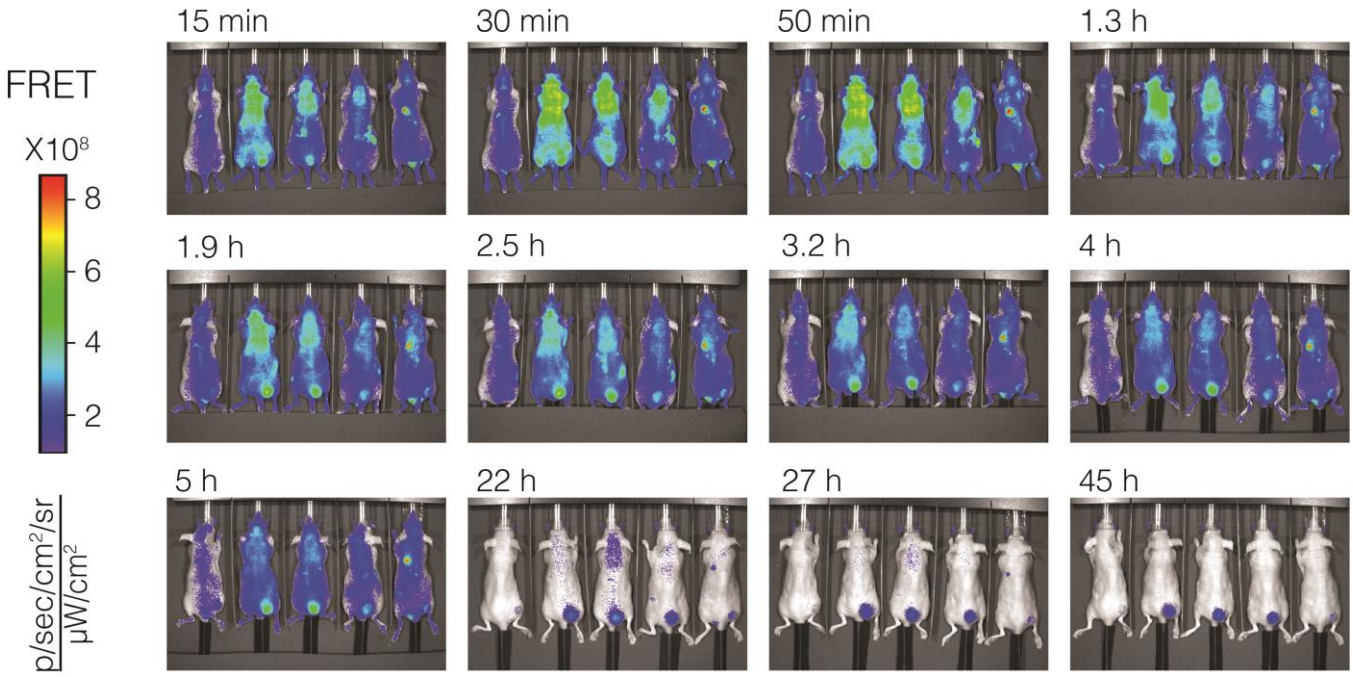

Figure S7. *in vivo* NIR florescence image of tumor-bearing mice intravenously injected with 100 pmol/g QD710-Cy7-PEG. At the indicated post-injection times, the fluorescence signal is collected through FRET channel (λ_{Exc}= 605± 18 nm, λ_{Em}= 800 ± 10 nm).

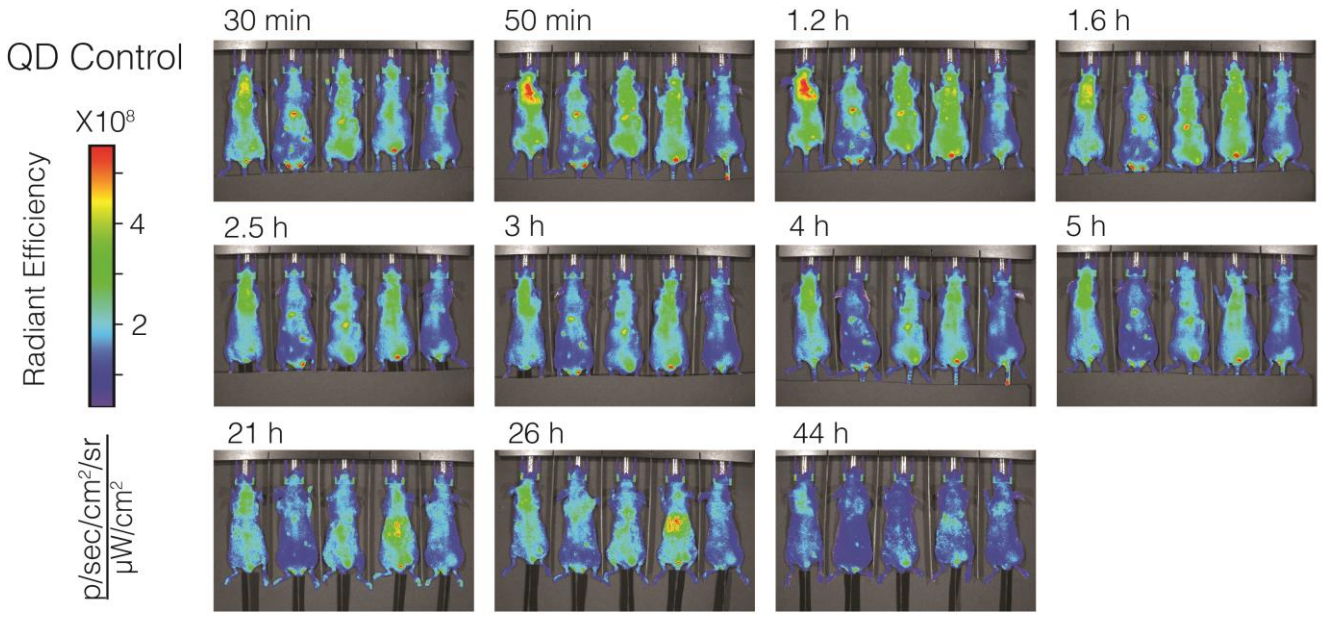

Figure S8 *in vivo* NIR florescence image of tumor-bearing mice intravenously injected with 100 pmol/g QD control QD710-PEG. At the indicated post-injection times, the fluorescence signal is collected through QD channel (λ_{Exc} = 605 ± 18 nm, λ_{Em} = 720 ± 10 nm).

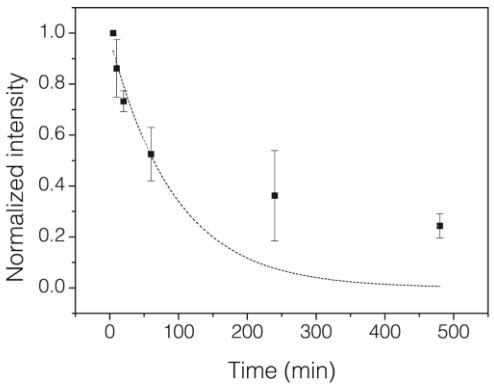

Figure S9. Circulation half-life analysis of QD610-PEG nanoparticles in nude mice. A single exponential fit (dashed line) gives the half-life value of QD720-PEG nanoparticles is about 65 ±11 min.

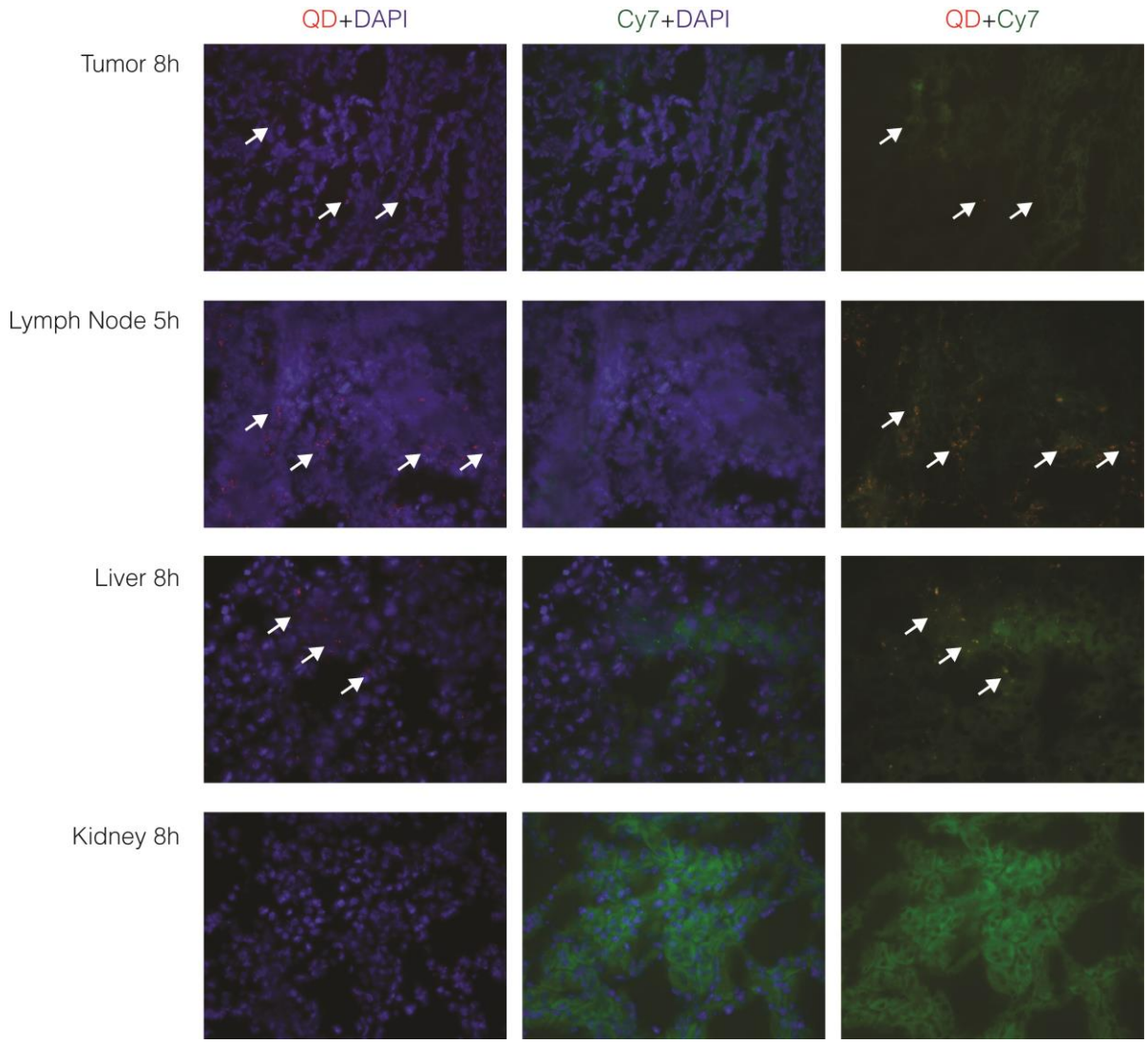

Figure S10. Fluorescence microscopy images of frozen sections of tumor, lymph node, liver and kidney tissues at 8 h post-injection. Signal from QD (λ_{Exc} = 620 ± 30 nm, λ_{Em}= 700 ± 35 nm) is presented in red, DAPI (λ_{Exc} = 350 ± 30 nm, λ_{Em}= 460 ± 22 nm) in blue and Cy7 (λ_{Exc} =710 ± 35 nm, λ_{Em}= 810 ± 40 nm) in green. Accumulated QDs are indicated by arrows.

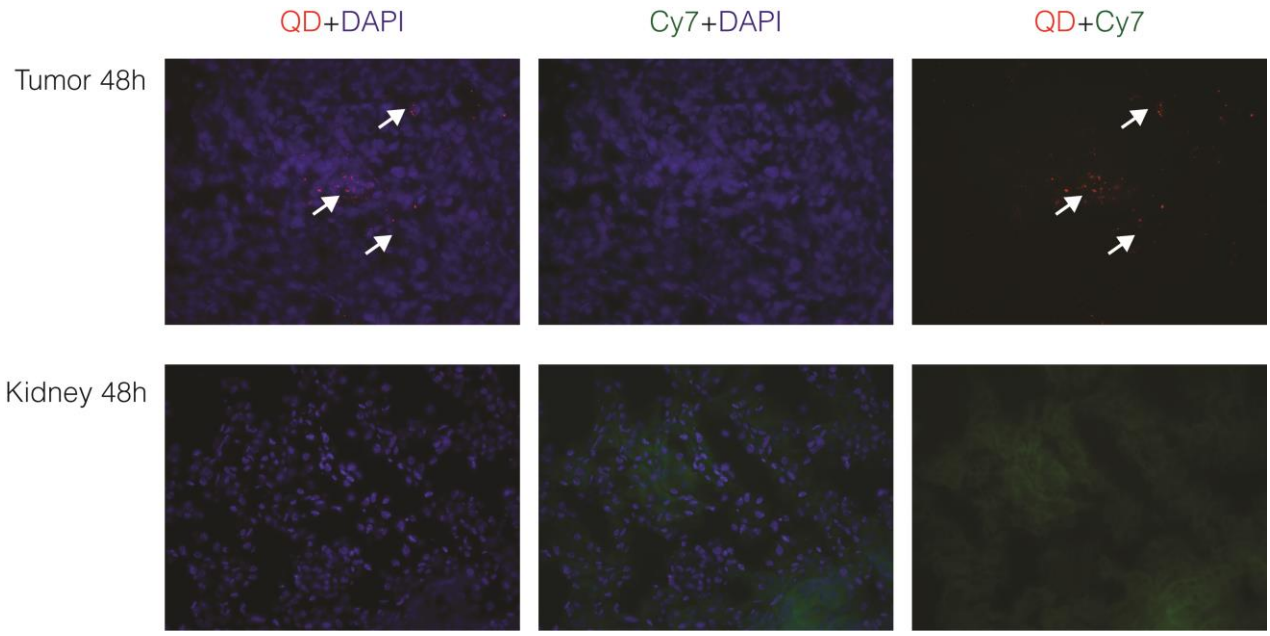

Figure S11. Fluorescence microscopy images of frozen sections of tumor and kidney tissues at 48 h post-injection. Signal from QD (λ_{Exc} = 620 ± 30 nm, λ_{Em}= 700 ± 35 nm) is presented red, DAPI (λ_{Exc} = 350 ± 30 nm, λ_{Em}= 460 ± 22 nm) in blue and Cy7 (λ_{Exc} =710 ± 35 nm, λ_{Em}= 810 ± 40 nm) in green. Accumulatied QDs are indicated by arrows.

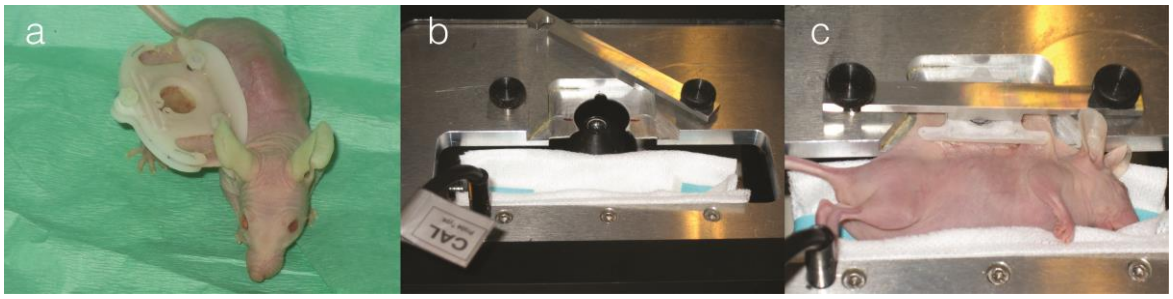

Figure S12. a, Tumor grown in dorsal window chambers in a nude mouse for intravital confocal laser scanning microscopy (CLSM). b, A custom build temperature-controlled CLSM imaging stage. c, Mouse with window chamber is loaded on the CLSM imaging stage.

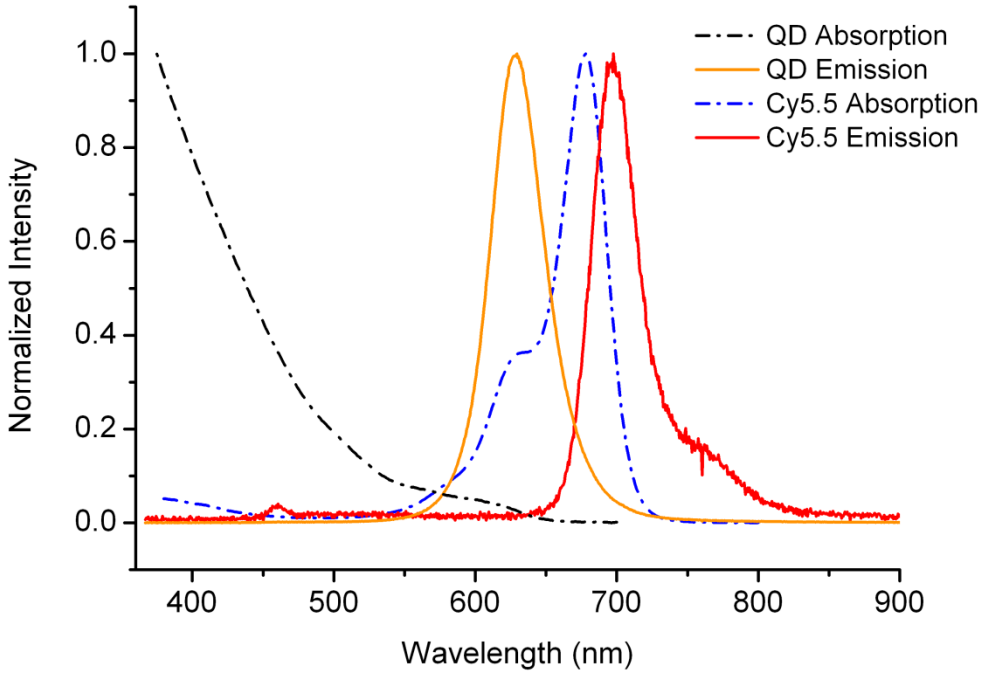

Figure S13. Absorption and emission spectra of QD610 and Cy5.5-lipids for QD610-Cy5.5-PEG nanoparticles.

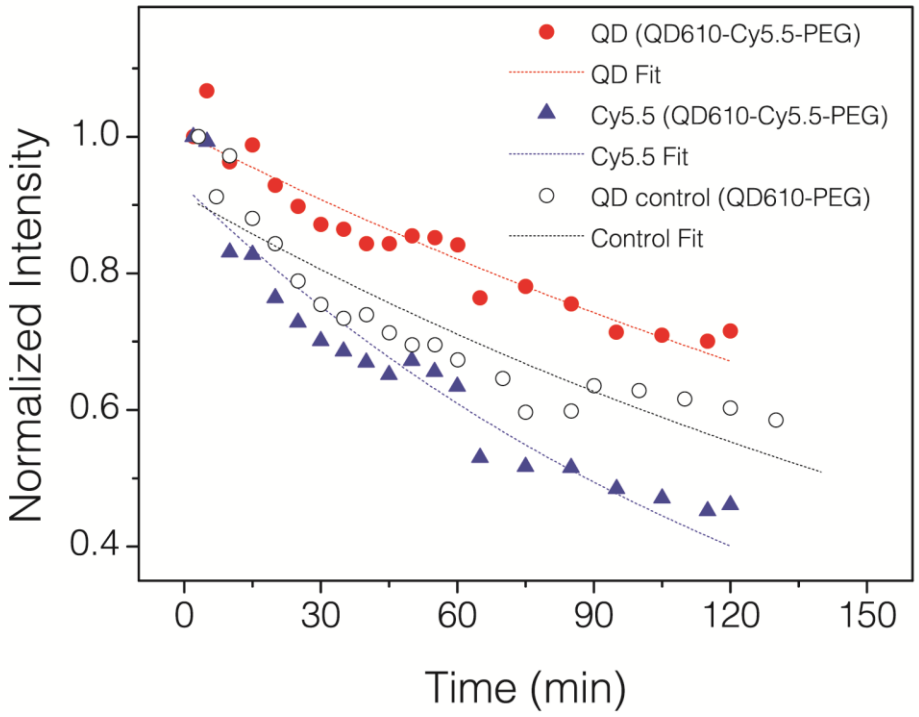

Figure S14. Biological half-life fitting on the data presented in Figure 3b. The fitting was based on a first order model $C_t = C_0 e^{-kt}$, where C_t is concentration after time t, C_0 is the initial concentration (t=0) and k is the elimination rate constant. The fitting results are presented in Table S1. Different components of the QD610-Cy5.5-PEG and QD610-PEG control have different circulation half-lives. Cy5.5 (circulation half-life 99 min) was cleared much faster than control QDs (166 min). The QD-Cy5.5-PEG dots appeared to have a much longer half-life (207 min) than control QDs due to the dequenching effect from the gradual disassociation of Cy5.5 lipids in the blood stream.

Table S1. Fitting results of biological half-life rate equation in Figure S11. Elimination half-life $t_{1/2}$ is calculated through relation $k = \ln 2 / t_{1/2}$.

	Elimination rate constant, k (min-1)	Elimination half-life $t_{1/2}$ (min)
QD (QD610-PEG)	4.17×10^{-3}	166
QD (QD610-Cy5.5-PEG)[a]	3.35×10^{-3}	207
Cy5.5 (QD610-Cy5.5-PEG)	6.99×10^{-3}	99

a. The elimination rate constant and half-life of QD610-Cy5.5-PEG determined from emission in QD channel is not the true half-live value of the nanoparticles. The dissociation of Cy5.5-lipids from QD core dequenches the QD emission, thus the half-life of QD610-Cy5.5-PEG appears longer than QD control, QD610-PEG.

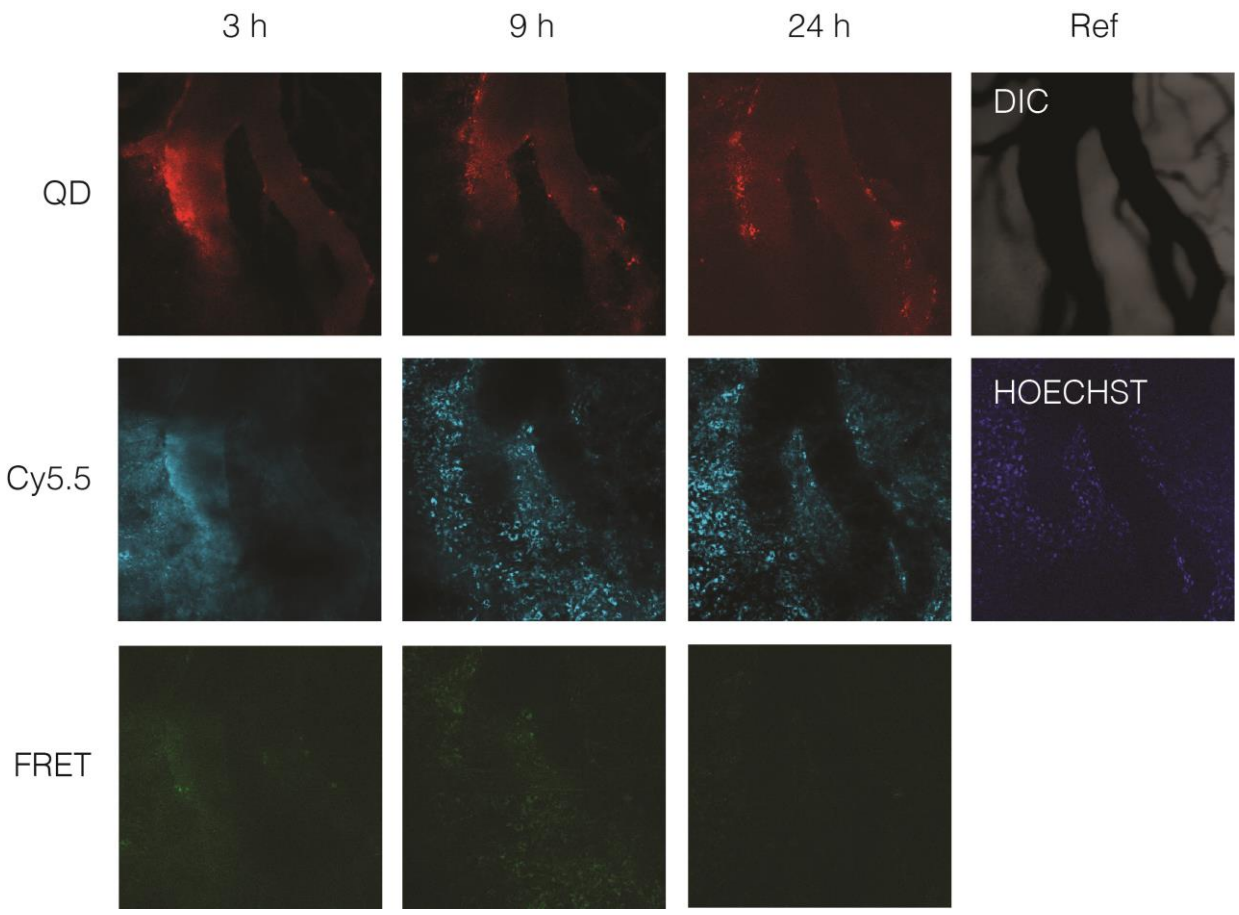

Figure S15. CLSM images of tumors grown in a window chamber model, after intravenous injection of 130 pmol/g QD610-Cy5.5-PEG. Images were recorded at 3, 9, 24 h post-injectionin three optical channels: QD (λ_{Exc} = 488 nm, λ_{Em}= 612-655 nm) are shown in red, Cy5.5 (λ_{Exc} = 633 nm, λ_{Em} = 698-719 nm) are shown in green, and FRET (λ_{Exc} = 488 nm, λ_{Em} = 698-719 nm) in cyan. HOECHST 33342 was injected 24 hours post injection of the nanoparticles to visualize cell nuclei facilitating the assessment of nanoparticle integrity and localization. HOECHST channel was excited with two photon excitation at 780 nm and detected with a bandpass filter at 435-485 nm.

References

1. Zhang, W.; Chen, G.; Wang, J.; Ye, B.C. and Zhong, X. Design and Synthesis of Highly Luminescent Near-Infrared-Emitting Water Soluble CdTe/CdSe/ZnS core/shell/shell Quantum Dots. *Inorg. Chem.* **2009**, 48, 9723-9731.
2. Wuister, S.F.; de Mello Donega, C. & Meijerink, A. Luminescence Temperature Antiquenching of Water-soluble CdTe Quantum Dots: Role of the Solvent. *J. Am. Chem. Soc.* **2004,** 126, 10397-10402.
3. Lim, J.; Jun, S.; Jang, E.; Baik, H.; Kim, H.; Cho, J. Preparation of Highly Luminescent Nanocrystals and Their Application to Light-Emitting Diodes. *Adv. Mater.* **2007,** 19, 1927-1912.
4. Clapp A. R.; Medintz I. L.; Mauro J. M.; Fisher B. R.; Bawendi M. G.; Mattoussi H., Fluorescence Resonance Energy Transfer Between Quantum Dot Donors and Dye-Labeled Protein Acceptors *J. Am. Chem. Soc.* **2004,** *126*, 301-310.